AIAA

Appendix 20 U. of Iowa 84-15

Theory of the Pulse Response from a Small Antenna in a Magnetized Plasma

by

CROCKETT L. GRABBE

Department of Physics and Astronomy
The University of Iowa
Iowa City, Iowa 52242

The electrostatic plasma response to a small pulsed antenna in a magnetic field is analyzed. The ringing of the plasma at three discrete frequencies--the upper-hybrid frequency and two resonance cone branch frequencies--is evidenced, and the amplitudes of these frequency responses is determined as a function of the characteristic plamsa frequencies, the angle of observation with respect to the magnetic field, and the pulse length. Applications to plasma diagnostics are discussed. It is show that the upper hybrid response and the response at either of the resonance cone branch frequencies is adequate information to determine the plasma density, and the magnetic field magnitude and angle.

I. INTROUDCTION

The problem of the radiated wave fields excited by small sources in magnetized plasmas has been of considerable interest in recent years because of the highly directional resonance cone nature of the waves under certain conditions [1,2]. In addition to being an interesting physical phenomena, resonance cones have been used as a diagnostic for density and temperature and form the channels along which power flows in certain radio frequency plasma heating experiments [3-5]. Most of the work on this subject has concentrated on continuous source plasma antennas.

The case of pulsed antennas is also of interest for a couple of reasons. First, the pulsed source can use less power than the continuous source, and this may be of importance in possible applications to plasma diagnostics, such as that of space plasmas observed on satellites and space vehicles. Second, for the continuous source case observation can only be made along the resonance cone angle, which is a function of the density and magnetic field, so that the angles must be swept to find the resonance cones in diagnostic applications. However, it may be of advantage to place the transmitting and receiving probes along a fixed direction.

An experiment has been performed on the wave response of a small pulsed antenna [6]. It was found that the response was a ringing at

three characteristic frequencies for any given angle θ of observation: the upper-hybrid frequency and two frequencies which correspond to the frequencies that would create the upper and middle branch of the resonance cones at a cone angle θ.

It is the purpose of this paper to develop the theory of the electrostatic response to a small pulsed antenna, which is done in Section II. The possible applications to diagnostics is discussed in Section III, and the results summarized in Section IV.

II. PULSE RESPONSE THEORY

We would like to solve the electrostatic Poisson's equations for a pulsed source. We will assume a cold plasma and a point source with a Gaussian time dependence centered about t = 0:

$$\nabla \cdot \mathbf{K} \cdot \nabla\phi(\vec{r},t) = \rho(\vec{r},t)/\varepsilon_0 \tag{1}$$

$$\rho(\vec{r},t) = q\delta(\vec{r})\, e^{-t^2/\tau^2} \quad , \tag{2}$$

where $\mathbf{K}$ is the plasma dielectric tensor and τ is the pulse length. We Fourier analyze these equations in space and Laplace transform in time to obtain

$$\tilde{\phi}(k,s) = \frac{-q}{\varepsilon_0} \frac{\int_{-\infty}^{\infty} e^{-t^2/\tau^2 - st}\, dt}{\vec{k} \cdot \mathbf{K}(s) \cdot \vec{k}} \quad , \tag{3}$$

where

$$\phi(x,t) = \int_{-\infty}^{\infty} \frac{d^3\vec{k}}{(2\pi)^3} \int_{\sigma-i\infty}^{\sigma+i\infty} \tilde{\phi}(k,s) e^{i\vec{k}\cdot\vec{r}+st}\, ds \quad . \tag{4}$$

The integral over t can be converted into the standard form for the conjugate error function (erfc) [7]. For the magnetic field in the z direction:

$$\bar{\bar{K}}(s) = \begin{bmatrix} K_\perp & iK_H & 0 \\ -iK_H & K_\perp & 0 \\ 0 & 0 & K_\parallel \end{bmatrix} , \tag{5}$$

where

$$K_\perp = 1 + \frac{\omega_{pe}^2}{s^2 + \omega_{ce}^2} + \frac{\omega_{pi}^2}{s^2 + \omega_{ci}^2} \tag{6}$$

$$K_\parallel = 1 + \frac{\omega_{pe}^2}{s^2} + \frac{\omega_{pi}^2}{s^2} \tag{7}$$

and K_H is the Hall term. These components reduce to the well-known form for $s \to -i\omega$. Choosing $\vec{k} = (k_x, 0, k_z)$, we can evaluate the inverse integral over k by well-known integral forms from Gradstein and Rhyzik [8] (see also Ref. [1]), or by rescaling of variables k_x and k_z:

$$\int_{-\infty}^{\infty} dk_x \int_{-\infty}^{\infty} dk_z \frac{e^{i(k_x r\sin\theta + k_z r\cos\theta}}{[k_x^2 K_\perp + k_z^2 K_\parallel]}$$

$$= \frac{1}{4\pi r} [(K_\perp^2 K_\parallel)(\sin^2\theta/K_\perp + \cos^2\theta/K_\parallel]^{-1/2} \quad . \tag{8}$$

Here θ is defined to be the angle between the magnetic field and the observation point (the group velocity angle). The inverse Laplace transform is then

$$\phi(\vec{r},t) = \frac{q\tau}{4\sqrt{\pi}\,\varepsilon_0 r} \int_{\sigma-i\infty}^{\sigma+i\infty} \frac{s(s^2 + \omega_{ce}^2)\mathrm{erfc}(\tau s/2)\exp(st+\tau^2 s^2/4)\,ds}{[(s^2 + \omega_1^2)(s^2 + \omega_2^2)(s^2 + \omega_{uh}^2)]^{1/2}} \quad , \tag{9}$$

where we have factored the denominator in Eq. (8), and

$$\omega_1(\theta) = \left\{\frac{\omega_{uh}^2}{2} - \left[\frac{\omega_{uh}^4}{4} - \omega_{pe}^2\omega_{ce}^2\sin^2\theta\right]^{1/2}\right\}^{1/2} \tag{10}$$

$$\omega_2(\theta) = \left\{\frac{\omega_{uh}^2}{2} + \left[\frac{\omega_{uh}^4}{4} - \omega_{pe}^2\omega_{ce}^2\sin^2\theta\right]^{1/2}\right\}^{1/2} \tag{11}$$

$$\omega_{uh} = (\omega_{pe}^2 + \omega_{ce}^2)^{1/2} \quad . \tag{12}$$

The first two frequencies are the middle and upper branch resonance cone frequencies, and ω_{uh} the upper-hybrid frequency. (Ion contributions are omitted.) These frequencies are plotted versus $\omega_{pe}^2/\omega_{uh}^2$ for various θ in Fig. 1. The conjugate error function erfc contains the pulse length dependence.

To evaluate the integral in Eq. (9), we pick the branch cuts and the Laplace integration contour as shown in Fig. 2. Now the quantity

erfc y e^{y^2} is a monotonically decreasing function of y with the small argument and asymptotic form

$$\text{erfc } y\, e^{y^2} \sim \begin{cases} \dfrac{1}{\sqrt{\pi}\, y} & (|y| \gg 1) \\ 1 & (|y| \ll 1) \end{cases} \tag{13}$$

Thus it is well behaved and contributes no singularities to the integral in Eq. (9). Hence we may use asymptotic techniques to evaluate the integral along the branch cuts. The integral over C_0 and the circle around the branch points are zero, while the sign change across each branch cut cause the integrals on each side of the branch cuts to be identical and additive. Thus we may parameterize each integration path along the branch cuts by $s = \pm i\omega_r - x$, where x is real:

$$\phi(r,t) = \frac{-q\tau}{2\sqrt{\pi}\,\varepsilon_0 r} \sum_{i=1}^{3} \sum_{\pm}$$

$$\times \int_0^\infty \frac{(\pm i\omega_i - x)[(\pm i\omega_i - x)^2 + \omega_{ce}^2]\,\text{erfc}[\tau/2(\pm i\omega_i - x)]\exp[\pm i\omega_i - x)t + (\pm i\omega_i - x)^2\tau^2]\,dx}{\{[(\pm i\omega_i - x)^2 + \omega_1^2][(\pm i\omega_i - x)^2 + \omega_2^2][(\pm i\omega_i - x)^2 + \omega_{uh}^2]\}^{1/2}} \tag{14}$$

At asymptotic times such that $e^{-\omega_i t} \ll 1$ for each ω, only the values of x such that $x \ll \omega_i$ will contribute significantly to the integral. This condition is satisfied for all three values of ω_i if $t \gg 1/\omega_1(\theta)$. Then by expanding to lowest order in x

$$\phi(r,t) \simeq \frac{-q\tau}{2\sqrt{\pi}\ \varepsilon_0 r} \sum_{i=1}^{3} \sum_{\pm} \frac{\sqrt{\pm 2i\omega_i}\ (\omega_{ce}^2 - \omega_i^2) e^{\pm i\omega_i t}\ \mathrm{erfc}(\pm i\omega_i \tau/2)}{[(\omega_j^2 - \omega_i^2)(\omega_k^2 - \omega_i^2)]^{1/2}}$$

$$\times \int \frac{e^{-xt}\, dx}{\sqrt{x}} + O(t^{-3/2})$$

$$\simeq \frac{-q\tau}{\varepsilon_0 r\ \sqrt{2t}} \sum_{\pm} \{A_h(\pm\omega_{uh}) e^{\pm i\omega_{uh} t} + A_2(\pm\omega_2) e^{\pm i\omega_2 t}$$

$$+ A_1(\pm\omega_1) e^{\pm i\omega_1 t}\} + O(t^{-3/2}) \quad , \tag{15}$$

where

$$A_h(\omega_{uh}) = \frac{-\sqrt{\omega_{uh}}\ \omega_{pe}^2\ w(\omega_{uh}\tau/2)}{[(\omega_{uh}^2 - \omega_1^2)(\omega_{uh}^2 - \omega_2^2)]^{1/2}} \tag{16}$$

$$A_2(\omega_2) = \frac{\sqrt{\omega_2}\ (\omega_{pe}^2 - \omega_2^2) w(\omega_2\tau/2)}{[(\omega_{uh}^2 - \omega_2^2)(\omega_2^2 - \omega_1^2)]^{1/2}} \tag{17}$$

$$A_1(\omega_1) = \frac{\sqrt{\omega_1}\ (\omega_{ce}^2 - \omega_1^2) w(\omega_1\tau/2)}{[(\omega_{uh}^2 - \omega_1^2)(\omega_2^2 - \omega_1^2)]^{1/2}} \quad . \tag{18}$$

Here w(y) is the w error function. (See Ref. 7, Chapter 7.) Also, $A_i(-\omega_i) = A_i^*(\omega_i)$. The form of the solution in Eq. (15) clearly shows the ringing of the plasma at the two resonance cone frequencies ω_1 and ω_2 and the upper-hybrid frequency ω_{uh}, as observed by Simmonutti [6]. The response dies away as $t^{-1/2}$. The magnitude of the amplitudes A_h, A_2, and A_1 are plotted in Figs. 3 and 4 as a function of $(\omega_{pe}^2/\omega_{uh}^2)$ for three angles of observation θ, and long and short pulse times τ.

III. PLASMA DIAGNOSTICS APPLICATION

By the use of transmitting and receiving probes in a plasma, one may measure through the use of a spectrum analyzer the three frequencies ω_1, ω_2 and ω_{uh} and their corresponding amplitudes A_1, A_2 and A_h. By comparing with the theoretical predictions given in Eqs. (10) - (12) and (16) - (18), one may deduce information on the plasma characteristics. We will show that this type of measurement is adequate to determine the plasma density, magnetic field strength, and magnetic field angle θ relative to the transmitting-to-receiving-antenna line in a plasma for which none of these is known.

Let us define the ratios

$$m_+ \equiv \frac{\omega_2}{\omega_{uh}} \qquad m_- \equiv \frac{\omega_1}{\omega_{uh}} \tag{19}$$

$$M_+ \equiv \frac{A_2}{A_h} \qquad M_- \equiv \frac{A_1}{A_h} \tag{20}$$

which are obtained from the primary measurements. Then put Eq. (12) into the form

$$\left(\frac{\omega_{ce}^2}{\omega_{uh}^2}\right) = 1 - \left(\frac{\omega_{pe}^2}{\omega_{uh}^2}\right) \quad . \tag{21}$$

Divide Eqs. (10) and (11) by ω_{uh}^2 and substitute Eq. (21) into them to obtain the two equations

$$\left(\frac{\omega_{pe}^2}{\omega_{uh}^2}\right)\left(1 - \frac{\omega_{pe}^2}{\omega_{uh}^2}\right) \sin^2\theta = 0.25[1 - (1 - 2m_{\pm}^2)^2]^{1/2} \quad . \tag{22}$$

Finally, evaluate the $M_{\pm}$ in Eq. (20) through Eqs. (16) - (18) to obtain the two equations

$$M_{\pm} = -\left[\frac{m_{\pm}(1 - m_{\mp}^2)}{|1 - 2m_{\pm}^2|}\right]^{1/2} \frac{(\omega_{ce}^2/\omega_{uh}^2 - m_{\pm}^2)w(\omega_{2,1}\tau/2)}{(\omega_{pe}^2/\omega_{uh}^2)w(\omega_{uh}\tau/2)} \quad . \tag{23}$$

Eqs. (22) and (23) form two independent equations for the two unknowns $(\omega_{pe}^2/\omega_{uh}^2)$ and θ, and Eq. (21) gives $(\omega_{ce}^2/\omega_{uh}^2)$ in terms of $(\omega_{pe}^2/\omega_{uh}^2)$. Since all other quantities are known through a measurement of the frequencies and their amplitudes, this is sufficient information to determine the plasma density (through $(\omega_{pe}$), magnetic magnitude (through ω_{ce}), and magnetic field angle θ. (With multiple receiving antennas we could narrow the magnetic field down to a unique direction.) But we have two sets of measurements, either one of which is adequate to determine these three quantities:

(1) M_+; ω_2, ω_{uh} and their ratio m_+.

(2) M_-; ω_1, ω_{uh} and their ratio m_-.

Thus we may use both sets of measurements in conjunction with each other to give two independent determinations of the plasma density and magnetic field angle and magnitude, and this will help improve the accuracy of the diagnostics.

Our model puts two conditions on the antenna that must be satisfied to ensure the validity of the results here for plasma diagnostic applications. First, the electrostatic approximation requires the transmitting antenna be of a monopole type (spherically symmetric) to guard against unwanted transverse wave components. Secondly, the antennas must be sufficiently small to be approximated by a delta function. Since $k_{min} \sim 2\pi/L$ where L is the antenna size and we require $\omega_{max} > \omega_{uh}$ and $(\omega/k) << c$, that means $L << 2\pi c/\omega_{uh}$ is the condition for that approximation. Both of these approximation requirements can easily be met for most applications.

IV. SUMMARY AND CONCLUSIONS

The plasma response to a pulsed plasma exhibits a discrete frequency response at the upper-hybrid frequency and the two resonance cone branch frequencies for the given angle of observation. The amplitude of these responses was calculated as a function of the various plasma and response frequencies, the observation angle, and the pulse length. These are summarized in Eqs. (16) - (18) and Figs. 2 and 3. A possible application of these results is to plasma diagnostics for the plasma density and magnetic field magnitude and angle. The determination of these quantities from pulse response measurements is carried out through Eqs. (21) - (23).

Some restrictions and limitations of the model used here were mentioned. The first is that a spherical antenna should be used to eliminate unwanted transverse wave components and ensure an electrostatic response. The second is that antenna sizes $L << 2\pi c/\omega_{uh}$ are required to make the delta function antenna configuration valid. Finally, thermal effects will modify the results in two ways. The first is that the cold plasma amplitudes blow up near $\theta = \pi/2$ and thus are not valid there. Thermal effects will limit those amplitudes. The second is that other plasma frequency responses will occur, such as the Bernstein and cyclotron harmonic wave resonances. Investigations of

thermal effects and finite antenna-size effects are planned for a future paper.

This research was sponsored by NASA grant NAG-364 and grant ATM-8312514 with the National Science Foundation.

REFERENCES

[1] R. Fisher and R. Gould, "Resonance cones in the field pattern of a radio frequency probe in a warm anisotropic plasma," Phys. Fluids, vol. 14, p. 857, 1971.

[2] H. Kuehl, "Interference structure near the resonance cone," Phys. Fluids, vol. 16, p. 1311, 1973.

[3] R. Briggs and R. Parker, "Transport of RF energy to the lower hybrid resonance in an inhomogeneous plasma," Phys. Rev. Lett., vol. 29, p. 852, 1972.

[4] C. Grabbe, "Energy flow and absorption along resonance cones near the lower hybrid," Phys. Fluids, vol. 22, p. 1323, 1979.

[5] P. Bellan and M. Porkolab, "Propagation and mode conversion of lower hybrid waves generated by a finite source," Phys. Fluids, vol. 17, p. 1592, 1974.

[6] M. Simmonutti, "Transient response froma small antenna in an anisotropic plasma," Phys. Fluids, vol. 19, p. 608, 1976.

[7] M. Abromowitz and L. Stegun, Handbook of Mathematical Functions. Washington, D.C.: National Bureau of Standards, 1964.

[8] I. Gradsteyn and I. Rhyzik, Table of Integrals, Series and Products. New York: Academic, 1965.

FIGURE CAPTIONS

Fig. 1. Integration contour for the inverse Laplace transform in Eq. (9). Branch cuts and branch points are indicated.

Fig. 2. Plots of the two resonance cone branch frequencies for three angles θ.

Fig. 3. Plots of the amplitudes of the upper-hybrid and resonance cone responses for three angles θ and a short pulse time.

Fig. 4. Plots of the amplitudes of the upper-hybrid and resonance cone responses for three angles θ and a long pulse time.

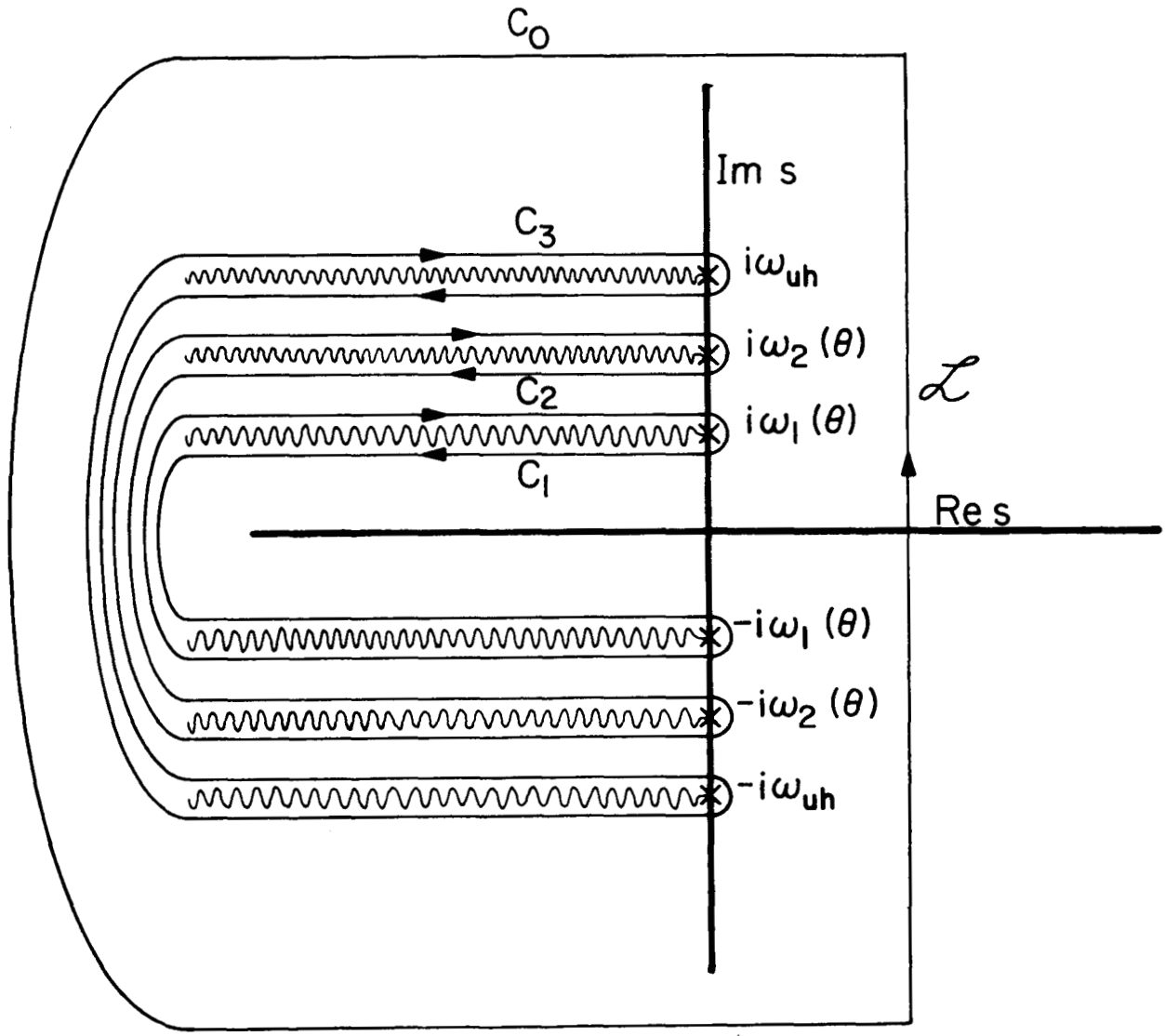
C_0
Im s
C_3
$i\omega_{uh}$
$i\omega_2(\theta)$
C_2
$i\omega_1(\theta)$
C_1
$\mathcal{L}$
Re s
$-i\omega_1(\theta)$
$-i\omega_2(\theta)$
$-i\omega_{uh}$

Fig. 1

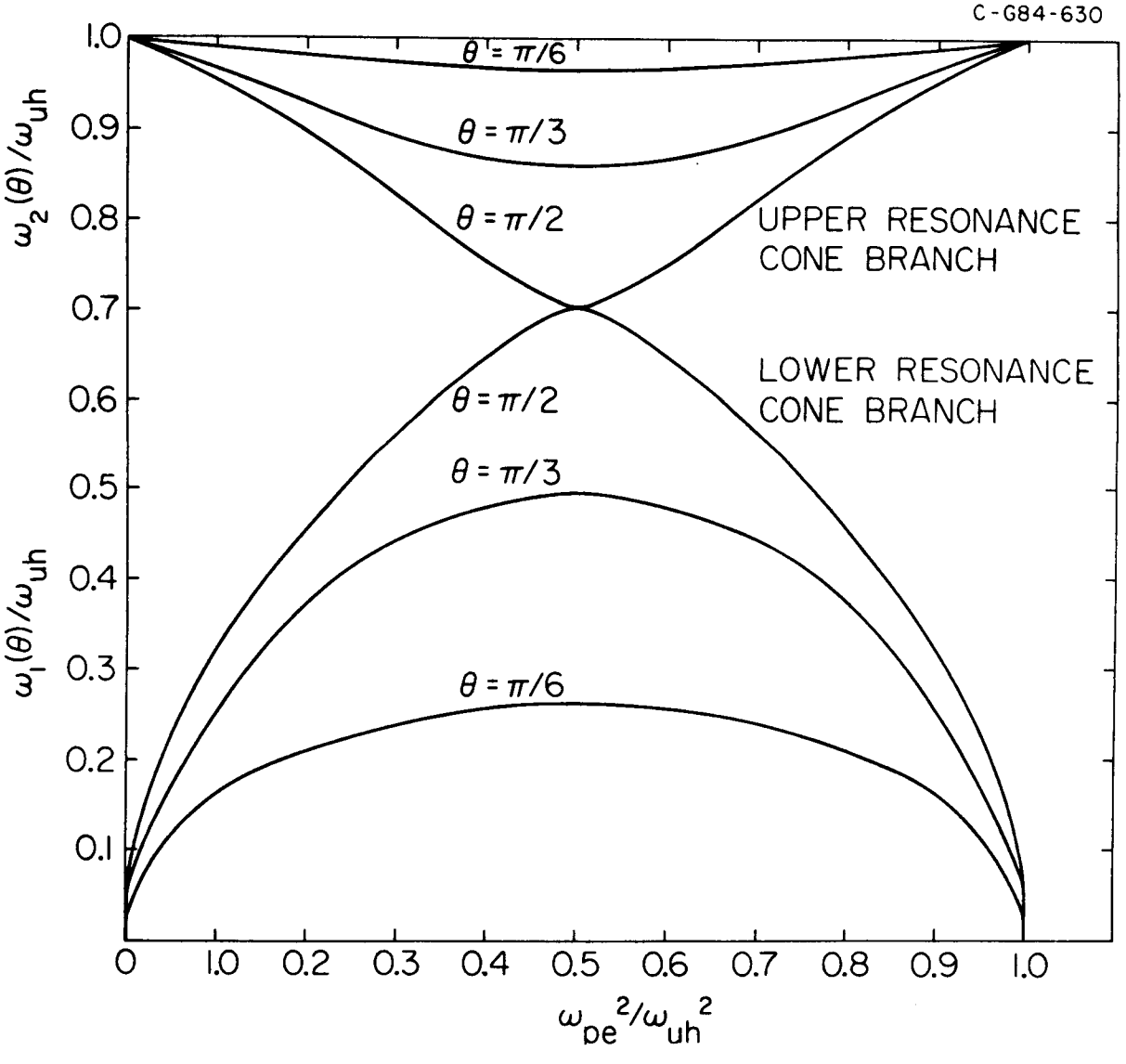
C-G84-630
1.0
0.9
0.8
0.7
0.6
0.5
0.4
0.3
0.2
0.1
0
1.0
0.2
0.3
0.4
0.5
0.6
0.7
0.8
0.9
1.0
$\omega_2(\theta)/\omega_{uh}$
$\omega_1(\theta)/\omega_{uh}$
$\omega_{pe}^2/\omega_{uh}^2$
$\theta = \pi/6$
$\theta = \pi/3$
$\theta = \pi/2$
UPPER RESONANCE CONE BRANCH
LOWER RESONANCE CONE BRANCH
$\theta = \pi/2$
$\theta = \pi/3$
$\theta = \pi/6$

Fig. 2

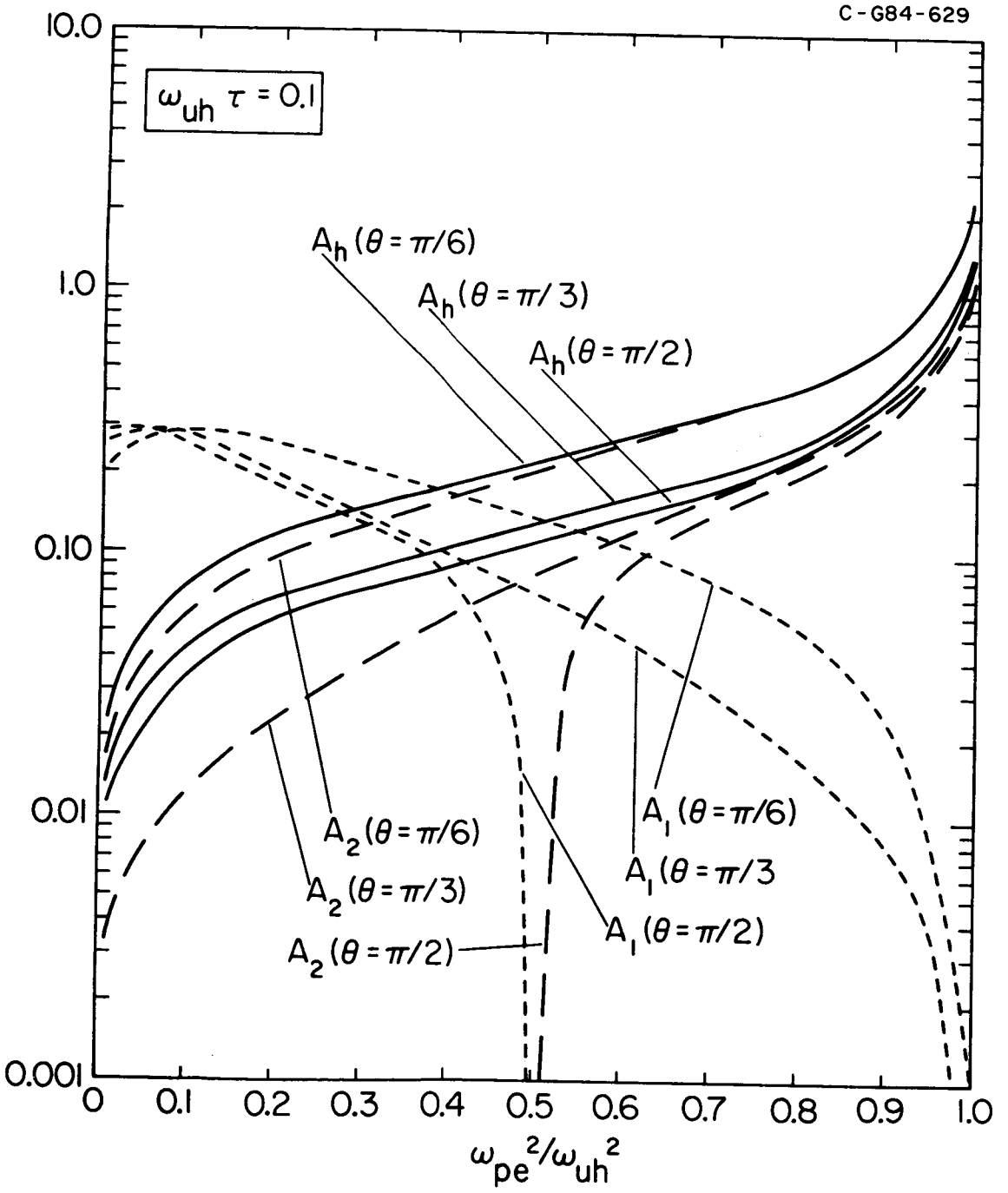
C-G84-629
$\omega_{uh}\,\tau = 0.1$
$A_h(\theta = \pi/6)$
$A_h(\theta = \pi/3)$
$A_h(\theta = \pi/2)$
$A_2(\theta = \pi/6)$
$A_2(\theta = \pi/3)$
$A_2(\theta = \pi/2)$
$A_1(\theta = \pi/6)$
$A_1(\theta = \pi/3$
$A_1(\theta = \pi/2)$
10.0
1.0
0.10
0.01
0.001
0
0.1
0.2
0.3
0.4
0.5
0.6
0.7
0.8
0.9
1.0
$\omega_{pe}^2/\omega_{uh}^2$

Fig. 3

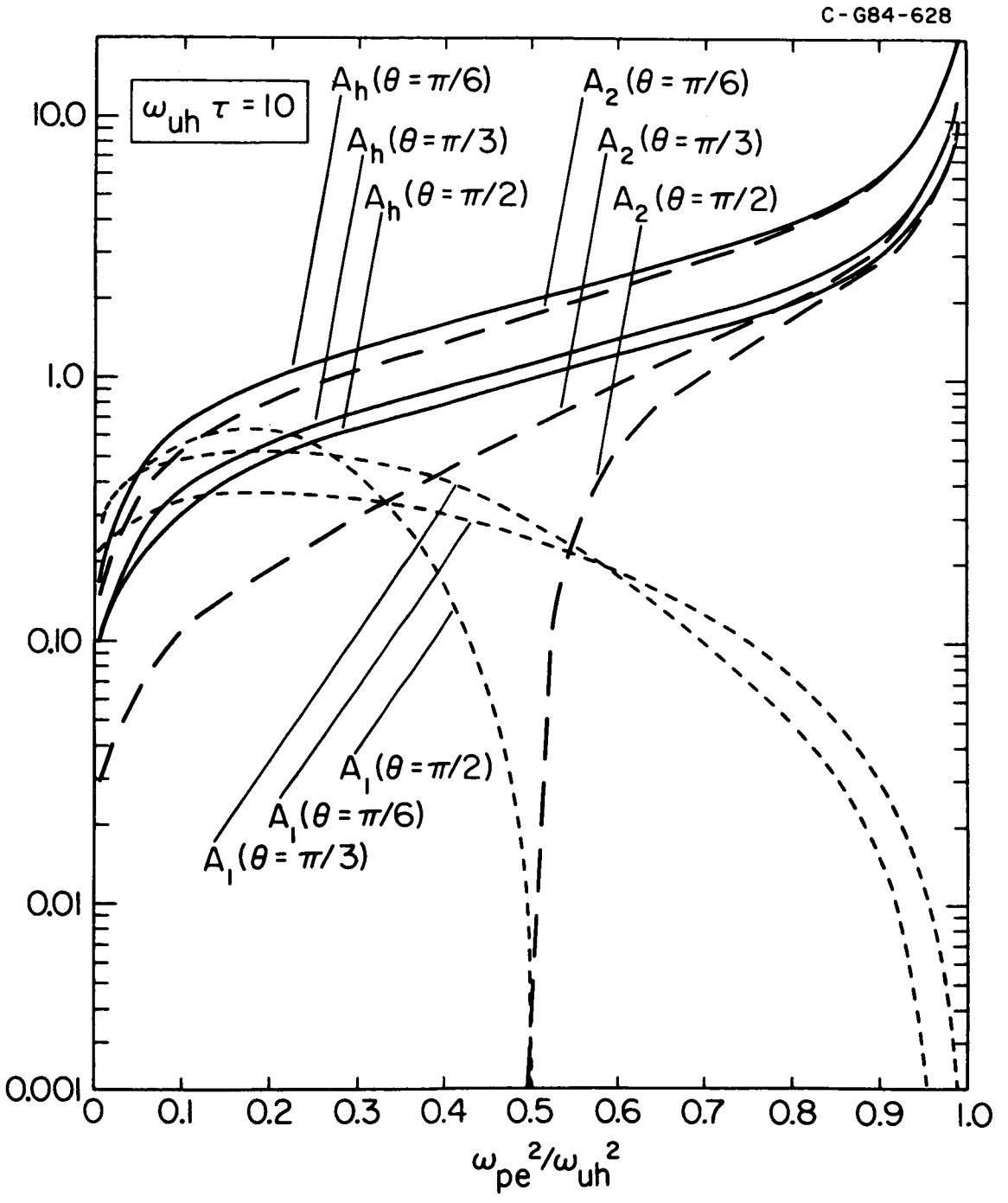
C-G84-628
$\omega_{uh}\tau = 10$
$A_h(\theta = \pi/6)$
$A_h(\theta = \pi/3)$
$A_h(\theta = \pi/2)$
$A_2(\theta = \pi/6)$
$A_2(\theta = \pi/3)$
$A_2(\theta = \pi/2)$
$A_1(\theta = \pi/2)$
$A_1(\theta = \pi/6)$
$A_1(\theta = \pi/3)$
10.0
1.0
0.10
0.01
0.001
0
0.1
0.2
0.3
0.4
0.5
0.6
0.7
0.8
0.9
1.0
$\omega_{pe}^2/\omega_{uh}^2$

Fig. 4